Supporting Information for

Self-Driven Pretreatment and Room-Temperature Storage of Water Samples for Virus Detection Using Enhanced Porous Superabsorbent Polymer (PSAP) Beads

Wensi Chen, Ting Wang, Zeou Dou, and Xing Xie[*]

School of Civil and Environmental Engineering, Georgia Institute of Technology, Atlanta, Georgia 30332, USA.

[*]Corresponding Author, E-mail: xing.xie@ce.gatech.edu

Table of Contents

1. Experimental Methods

1.1 One-step RT-qPCR Procedures

One-step quantitative reverse transcription PCR (RT-qPCR) assay was performed with StepOnePlus real-time PCR using the iTaq universal probes one-step kit (Bio-Rad, Hercules, CA).[1] The oligonucleotide sequences of a primer pair and a fluorogenic probe were designed to detect a gene encoding the maturation protein (A-protein) of bacteriophage MS2 (Table S2). In brief, 5 μL of the extracted and purified RNA was mixed with iTaq reaction mixture, reverse transcriptase, primers, and probe to reach a final volume of 20 μL following the manufacturer's instructions. The thermal cycling condition for the one-step RT-qPCR is as follows: 50°C for 10 min (reverse transcription reaction), 95°C for 2 min (polymerase activation and DNA denaturation), and then 40 cycles of 95°C for 5 s and 60°C for 30 s (amplification). The standard curve for quantification of viral RNA shown in Figure S6 was established using the synthesized RNA oligonucleotides of bacteriophage MS2 (sequence position: 629-711). All oligonucleotides were purchased from Integrated DNA Technologies, Inc. (Coralville, IA) and used as received without further purification.

1.2 Bacterial Rejection Test

The bacterial rejection performance of the PSAP beads with different stabilizer loadings was demonstrated using a Gram-negative bacterium, *Escherichia coli* (*E. coli*, ATCC 15597), and a Gram-positive bacterium, *Staphylococcus epidermidis* (*S. epidermidis*, ATCC 12228). The bacteria were cultured in sterilized broth (Luria-Bertani broth for *E. coli* and nutrient broth for *S. epidermidis*) to log phase and harvested by centrifugation at 4000 rpm. After washing with DI water for three times, the bacterial suspension containing *E. coli* or *S. epidermidis* was diluted in the saline medium (0.1% NaCl) to achieve a desired concentration of ~500 CFU mL^{-1}. A total of 10 PSAP beads were applied to treat 2 mL of bacteria sample, and the hydrated beads were subsequently taken out after 15 min treatment. The volumes of the original and residual liquid samples were V_0 and V_r, respectively. The bacterial concentrations before and after the treatment (c_0 and c_r) were measured using the standard spread plating method with three replicates for each measurement. Therefore, the bacterial rejection efficiency was determined as follows: $Rejection(\%)=(c_rV_r-c_0V_r)/(c_0V_0-c_0V_r)\times100$. Imaging and analysis of the bacteria attached to the PSAP beads were performed with confocal fluorescence microscopy (Zeiss, Oberkochen,

Germany). To better observe the distribution of the bacteria cells, the bacteria suspension with a high cell density (~10^9 CFU mL^{-1}) was stained by SYTO 9 dye (6 μM) for 20 min before the PSAP treatment. The fluorescence intensity from the surface to the core of the hydrated PSAP bead was analyzed and normalized, in which the maximum fluorescent intensity at the bead surface was set as the baseline.

2. Additional Results and Discussion

2.1 Effects of Light Exposure on Viral Shelf Life

To investigate the light effects on the viral shelf life, we conducted similar storage experiments at room temperature (22℃) with 12 hours of indoor light illumination every day. The data collection and analysis procedures were similar to the dark storage experiments. As shown in Figure S3a, the light has a relatively minor impact on the viral inactivation compared with the temperature, in which the viral inactivation rate slightly increases under the light exposure. Although the efficacy is affected a little, the PSAP beads can still protect viral infectivity under light conditions. The beads with 0.05% BSA provide a 7-day viral survival rate of 1.4%, which is increased to 8.5% and 36% at the BSA loading of 0.1% and 0.2%, respectively. Comparing the dark- and light-storage results at the same temperature, the viral infectivity reduction caused by the light exposure is less significant in all PSAP groups than in the liquid control group, regardless of the BSA loading amount. It is probably because the hydrated PSAP beads can block part of the light, and avoid or reduce photo-induced inactivation reactions (*e.g.*, generation of reactive oxygen species). At the same storage temperature with light exposure, the rate constant varies from 0.385 to 0.058 $\log_{10}$ PFU mL^{-1} day^{-1}, depending on the BSA loading (Figure S3b). Overall, these experimental results indicate a clear improvement of viral infectivity using the PSAP bead entrapment over maintaining the sample in the liquid state for the duration of the study.

2.2 Bacterial Rejection Performance

Based on the rational design, the optimal PSAP beads should achieve both a high recovery efficiency for viruses and a high rejection efficiency for undesired large impurities. To investigate the bacterial rejection performance, the PSAP beads were applied to treat a saline medium containing *E. coli* (Gram-negative bacterium with a size of 1-2 μm) or *S. epidermidis* (Gram-positive bacterium with a size of 0.5-1.5 μm). Figure S5a shows the rejection efficiency for *E. coli* and *S. epidermidis* after the PSAP treatment, respectively. For *E. coli* rejection, the pristine PSAP beads with 0% BSA show a rejection of 95%, which means at least 95% of *E. coli* cells are excluded outside the PSAP beads. As the BSA loading increases from 0.05% to 0.3%, the rejection efficiency of the PSAP beads for *E. coli* remains at a high level (>90%), which suggests the rejection of bacterial cells is not affected by the existence of the BSA even at relatively high loading. For *S. epidermidis* rejection, the efficiency is slightly lower, in which the pristine beads

show a rejection of 82%. In our calculation, the surface-attached bacterial cells on the hydrated beads after PSAP treatment are not included in the excluded cells for rejection calculation. Due to their smaller size, *S. epidermidis* may be more easily attach to the pore structures and remain on the bead surface, which causes a lower rejection efficiency compared with *E. coli*. Nevertheless, all PSAP beads can still achieve higher than 80% *S. epidermidis* rejection. The results indicate that the BSA modification improves the absorption of viruses without sacrificing bacteria rejection. For undesired large components within a certain range, the exclusion performance is mainly determined by the size effects, and thus the rejection efficiency slightly decreases with the decreased particle size. Meanwhile, the loading of the BSA doesn't have a significant influence on bacterial rejection and will not increase the surface attachment of bacterial cells.

As mentioned, a few bacterial cells may attach to the bead surface after the PSAP treatment. We expected these bacteria only left on the beads surface and would have no impact on the absorbed viruses. To confirm this, the fluorescence microscopy together with stained *E. coli* cells was applied to observe and visualize the distribution of bacterial cells on the bead surface and/or inside the beads after the PSAP treatment. Figure S5b presents that most of the bacterial cells are excluded outside the bead, while only a few are attached to the surface and nearly no bacterial cells enter the bead. To further investigate the distribution of bacteria on the bead surface, confocal fluorescence microscopy was applied to detect stained *E. coli* cells from the surface toward the center of the PSAP bead. Figure S5c shows the 3D reconstruction image of the bacterial cells distributed in the bead, which indicates that the bacterial density gradually decreases with increasing depth. To quantify the bacterial density variation, the fluorescence intensity of each layer (*i.e.*, the bacterial density at a certain depth) was integrated and normalized to the value obtained for the outmost layer of the bead. As illustrated in Figure S5d, the normalized fluorescence intensity predictably drops as the bead depth increases, which is only 0.2 at a depth of 5 μm and reaches almost zero at a depth of 10 μm. This penetration depth of bacterial cells to the beads (10 μm) is negligible compared with the whole size of the hydrated beads (~5 mm in diameter). These results indicate that although a few large impurities such as bacteria may be left on the PSAP surface after the treatment, these undesired components are restricted to the surface level and almost cannot enter the bead. Therefore, the viruses stored inside the PSAP beads will not be affected by these undesired components.

3. Additional Figures

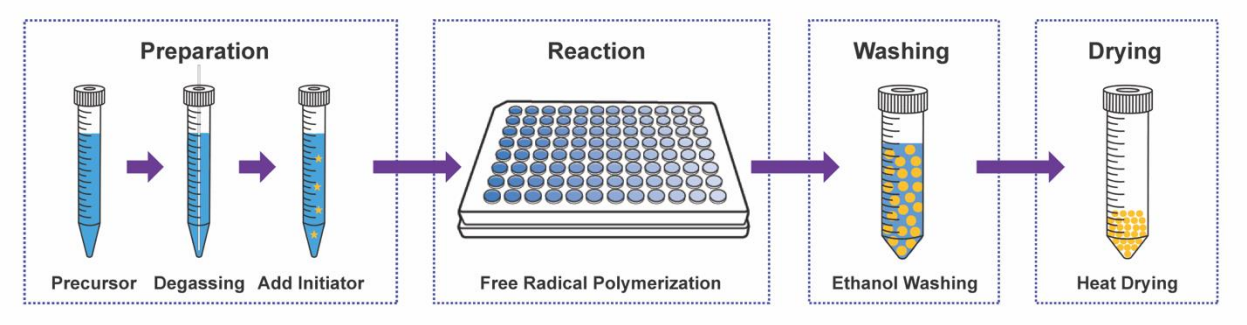

Figure S1. Schematic of the synthesis process for the PSAP beads.

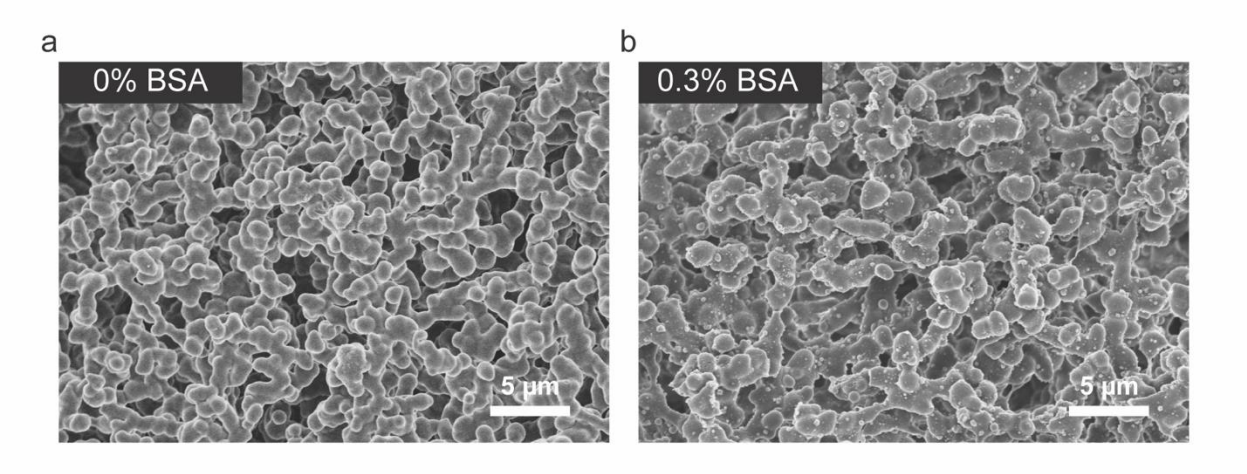

Figure S2. SEM images of the PSAP beads modified with different amounts of BSA stabilizer.

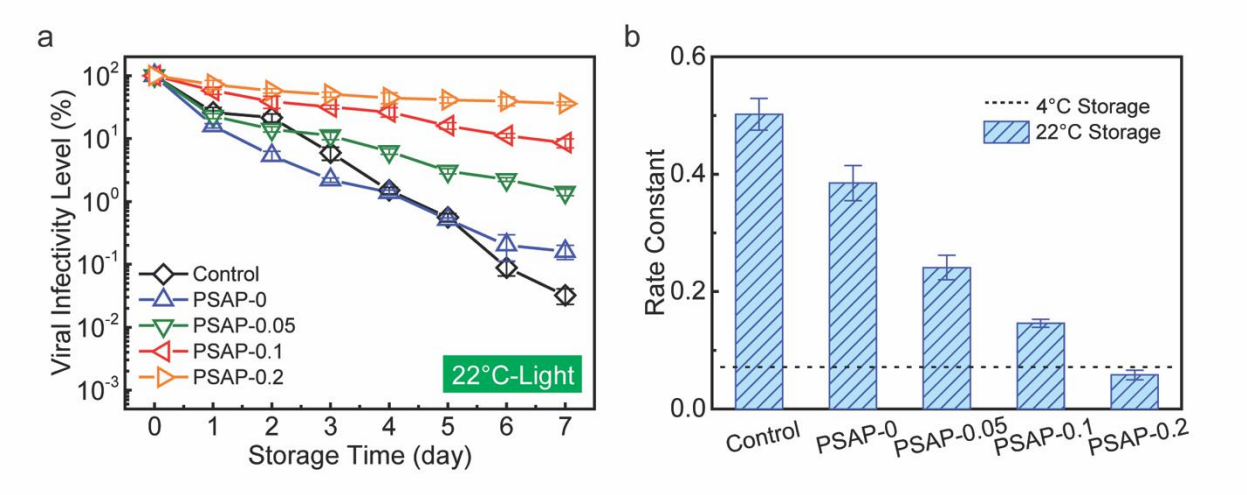

Figure S3. Shelf-life extension of bacteriophage MS2 using the PSAP beads with light exposure. (a) Normalized viral infectivity in liquid control and hydrated PSAP beads at room temperature. The legend "PSAP-0" means the PSAP beads with 0% BSA, which applies to similar legends. (b) Rate constants for viral infectivity reduction (k, $\log_{10}$ PFU mL^{-1} day^{-1}) during the 7-day storage. The black dotted line in (b) indicates the rate constant of the liquid sample stored at 4℃ in dark environment.

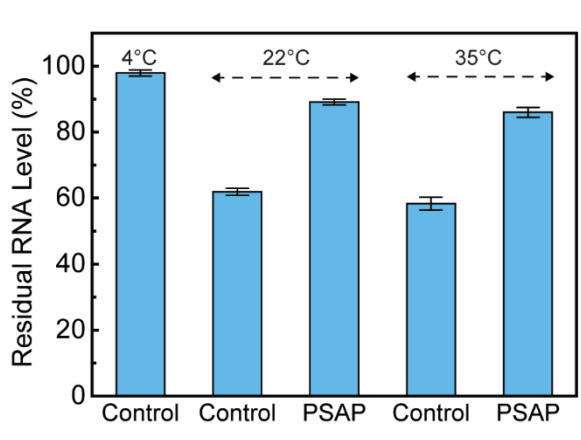

Figure S4. Residual RNA level of the naked RNA in liquid control and PSAP beads after 1-week storage. The PSAP beads used were modified with 0.2% BSA. The synthesized RNA oligonucleotide based on the sequence of bacteriophage MS2 genome (position: 629-711) was dispersed in saline medium (0.1% NaCl) to reach an initial concentration of ~10^6 copies mL^{-1}.

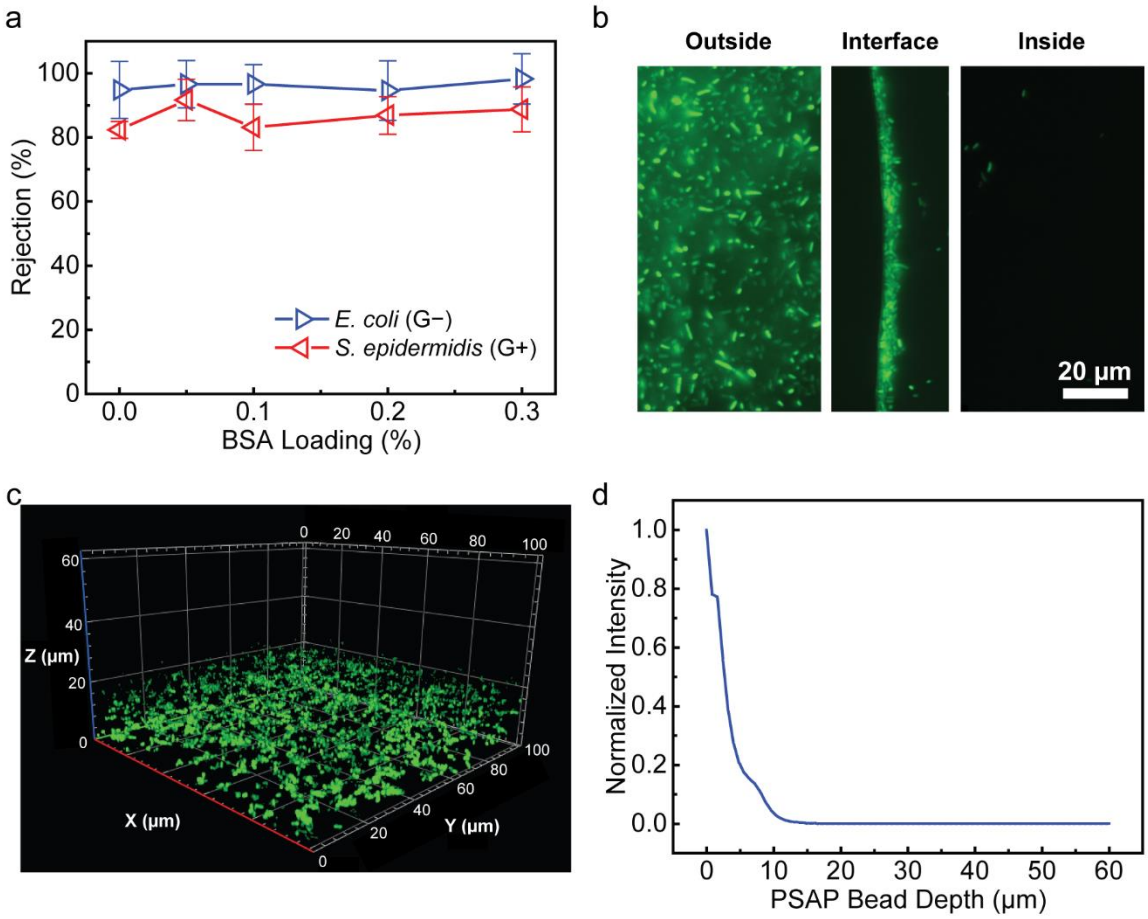

Figure S5. Bacterial rejection performance of the PSAP beads. (a) Rejection efficiency for bacteria. (b) Fluorescence microscopy images of the external surface and cross-section of the PSAP beads after the treatment. The bacteria used were *E. coli* cells stained by SYTO 9. (c) Distribution of stained bacterial cells on the PSAP surface. The xy-plane is aligned to the layer of the bead at a certain depth. The z-axis corresponds to the depth into the bead. The outermost surface of the bead was set at z=0. (d) Normalized fluorescence intensity on the surface level of the PSAP bead after the treatment.

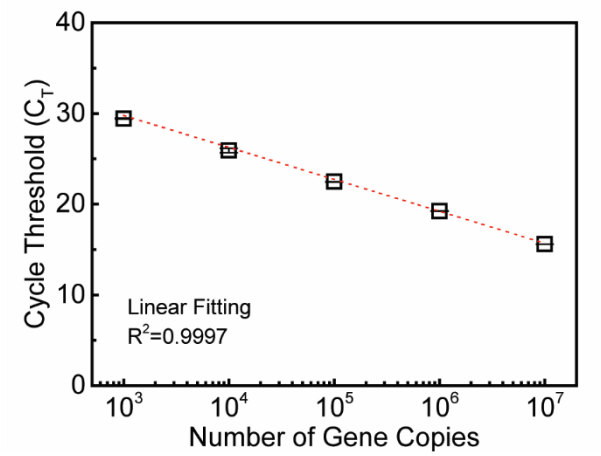

Figure S6. Standard curve for the quantification of viral RNA.

4. Additional Tables

Table S1. General properties of the untreated wastewater

Item	pH	Ortho Phosphorus (mg L^{-1})	Ammoniacal Nitrogen (mg L^{-1})	Nitrate (mg L^{-1})	Alkalinity (mg L^{-1} $CaCO_3$)	Total Suspended Solids (mg L^{-1})
Untreated Wastewater[a]	7.65	5.6	34.6	0.458	201	342

[a]The untreated wastewater was collected from a local wastewater treatment plant in Georgia, USA.

Table S2. Oligonucleotide sequences of the primer pair and probe used for detection of bacteriophage MS2 in real-time qPCR

Primers and Probe	Oligonucleotide Sequence	Base Pair	GC Content	Position
Forward Primer	5′-GTC GCG GTA ATT GGC GC-3′	17	64.7%	632-648
Reverse Primer	5′-GGC CAC GTG TTT TGA TCG A-3′	19	52.6%	690-708
TaqMan Probe	5′-AGG CGC TCC GCT ACC TTG CCC T-3′	22	68.2%	650-671

Reference

1. Rattanakul, S.; Oguma, K., Analysis of hydroxyl radicals and inactivation mechanisms of bacteriophage MS2 in response to a simultaneous application of UV and chlorine. *Environmental science & technology* **2017,** *51* (1), 455-462.